Clinical Science (2016) **130**, 711–720 doi: 10.1042/CS20150838

Original Paper

Mapping time-course mitochondrial adaptations in the kidney in experimental diabetes

Melinda T. Coughlan*†‡, Tuong-Vi Nguyen*, Sally A. Penfold*, Gavin C. Higgins*§, Vicki Thallas-Bonke*, Sih Min Tan*†, Nicole J. Van Bergen‖, Karly C. Sourris*†, Brooke E. Harcourt¶, David R. Thorburn¶, Ian A. Trounce‖, Mark E. Cooper*† and Josephine M. Forbes*,**††

*Glycation, Nutrition & Metabolism Laboratory, Baker IDI Heart & Diabetes Institute, Melbourne, Victoria 8008, Australia
†Department of Medicine, Central Clinical School, Monash University, Alfred Medical Research & Education Precinct, Melbourne, Victoria 3004, Australia
‡Department of Epidemiology & Preventive Medicine, Monash University, Alfred Medical Research & Education Precinct, Melbourne, Victoria 3004, Australia
§Department of Biochemistry & Molecular Biology, Monash University, Clayton, Victoria 3800, Australia
‖Centre for Eye Research Australia, Eye and Ear Hospital, East Melbourne, Victoria 3002, Australia
¶Murdoch Children's Research Institute, Royal Children's Hospital, Parkville, Victoria 3052, Australia
**Glycation and Diabetes, Mater Research Institute-The University of Queensland, TRI, South Brisbane, QLD 4102, Australia
††School of Medicine, Mater Clinical School, The University of Queensland, St Lucia, QLD 4067, Australia

Abstract

Oxidative phosphorylation (OXPHOS) drives ATP production by mitochondria, which are dynamic organelles, constantly fusing and dividing to maintain kidney homoeostasis. In diabetic kidney disease (DKD), mitochondria appear dysfunctional, but the temporal development of diabetes-induced adaptations in mitochondrial structure and bioenergetics have not been previously documented. In the present study, we map the changes in mitochondrial dynamics and function in rat kidney mitochondria at 4, 8, 16 and 32 weeks of diabetes. Our data reveal that changes in mitochondrial bioenergetics and dynamics precede the development of albuminuria and renal histological changes. Specifically, in early diabetes (4 weeks), a decrease in ATP content and mitochondrial fragmentation within proximal tubule epithelial cells (PTECs) of diabetic kidneys were clearly apparent, but no changes in urinary albumin excretion or glomerular morphology were evident at this time. By 8 weeks of diabetes, there was increased capacity for mitochondrial permeability transition (mPT) by pore opening, which persisted over time and correlated with mitochondrial hydrogen peroxide (H_2O_2) generation and glomerular damage. Late in diabetes, by week 16, tubular damage was evident with increased urinary kidney injury molecule-1 (KIM-1) excretion, where an increase in the Complex I-linked oxygen consumption rate (OCR), in the context of a decrease in kidney ATP, indicated mitochondrial uncoupling. Taken together, these data show that changes in mitochondrial bioenergetics and dynamics may precede the development of the renal lesion in diabetes, and this supports the hypothesis that mitochondrial dysfunction is a primary cause of DKD.

Key words: diabetic nephropathy, experimental diabetes, kidney disease, mitochondria.

INTRODUCTION

Chronic kidney disease (CKD) is a major risk factor for cardiovascular events and all-cause mortality [1], affecting more than 50 million individuals world wide [2]. CKD incidence is projected to dramatically increase over the next two decades, particularly in developing nations, as a result of key risk factors including hypertension, diabetes and associated cardiovascular disease [3]. Hence, preventing the onset or progression of CKD is likely to significantly reduce all-cause mortality across many populations. At least 30–40% of the burden of CKD is as a result of diabetes [4], although not all diabetic individuals will develop kidney disease, suggesting that there is an underlying genetic predisposition to this disorder [5]. Of the minority of patients with CKD who

Abbreviations: BW, body weight; CKD, chronic kidney disease; CsA, cyclosporin A; DKD, diabetic kidney disease; GHb, glycated haemoglobin; GSI, glomerulosclerotic index; KIM-1, kidney injury molecule-1; Mff, mitochondrial fission factor; Mfn, mitofusin; MnSOD, manganese superoxide dismutase; mPT, mitochondrial permeability transition; mtDNA, mitochondrial DNA; mt(nDNA), mitochondrial nuclear-encoded DNA; nDNA, nuclear DNA; OCR, oxygen consumption rate; OPA1, GTPase optic atrophy-1; OXPHOS, oxidative phosphorylation; PAS, periodic acid–Schiff; PTEC, proximal tubule epithelial cell; ROS, reactive oxygen species.

Correspondence: Professor Melinda T. Coughlan (email Melinda.Coughlan@bakeridi.edu.au).

© 2016 Authors; published by Portland Press Limited

do not eventually die from a cardiovascular event, many will progress to end-stage renal disease and require renal transplantation or dialysis. Along with management of hyperglycaemia and hypertension, agents which target the renin–angiotensin system are widely used in clinical practice in patients with diabetic kidney disease (DKD). Despite this, renal function still progressively declines in the majority of patients [6]. Clearly, there is a critical need to identify the pathogenic factors that lead to the onset and progression from DKD to cardiovascular and end-stage renal disease in order to develop novel therapeutic targets.

Mitochondria are fundamental to metabolic homoeostasis by converting nutrient flux into ATP via the process of oxidative phosphorylation (OXPHOS). Normal kidney function is energetically demanding, and the proximal tubule of the kidney generates vast quantities of ATP via OXPHOS to facilitate active reabsorption of macromolecules [7]. Many lines of evidence suggest that mitochondrial dysfunction and bioenergetic defects play a central role in the development of DKD [8–15]; with mitochondrial ATP depletion and mitochondrial uncoupling features of disrupted mitochondrial homoeostasis. A clear link between DKD and a shift in mitochondrial dynamics has also recently emerged from studies demonstrating mitochondrial fragmentation in the diabetic kidney [16–18]; however, whether these changes in mitochondrial dynamics and bioenergetics are present prior to the development of early renal structural and biochemical lesions remains unknown.

To address this issue, we used a streptozotocin-induced diabetic rat model, which allowed us to study early changes in the kidney that are difficult to map in individuals with diabetes. This well-established model of diabetes complications has most hallmarks of progressive human DKD including hyperfiltration, albuminuria and renal structural defects. Hence we could study temporal changes in renal function and morphology and link these to adaptive mechanisms in mitochondria, in particular mitochondrial function and structure.

MATERIALS AND METHODS

Experimental animal model

All animal experiments were performed in accordance with guidelines from the Alfred Medical Research and Education Precinct Animal Ethics Committee and the National Health and Medical Research Council of Australia. Animals were housed in groups of three rats per cage in a temperature-controlled environment, with a 12 h light/12 h dark cycle and *ad libitum* access to food and water. Experimental diabetes was induced in 6-week-old male Sprague–Dawley rats (200–250 g) by intravenous injection of streptozotocin (50 mg/kg in sodium citrate buffer, pH 4.5) following an overnight starving [19]. Animals with plasma glucose concentrations in excess of 15 mmol/l at 1-week post induction of diabetes were included in the study. Diabetic and control animals were randomized into groups ($n = 10$ per group) and followed for 4, 8, 16 or 32 weeks. Insulin (Humalog, Eli-Lilly) (2–3 units) was administered daily to diabetic animals to prevent ketoacidosis and improve survival. At 24 h before the study time-points, rats were placed individually into metabolic cages (Iffa Credo). Blood glucose was measured using a glucometer (Accutrend; Boehringer Manheim Biochemica). Glycated haemoglobin (GHb) was determined by a Cobas Integra 400 autoanalyzer (Roche Diagnostics Corporation). At the specified time-points, animals were killed and the kidneys were rapidly dissected, weighed and snap-frozen or placed in 10% (v/v) neutral buffered formalin for fixation before paraffin embedding. In a subset of rats ($n = 5$ per group), mitochondria were isolated from fresh renal cortices as described below. Renal cortices from five rats per group were processed for transmission electron microscopy as described below.

Renal function and morphometry

Rat-specific ELISAs were used to measure urinary albumin excretion (Bethyl Laboratories), urinary kidney injury molecule-1 (KIM-1; USCN Life Sciences) and serum cystatin C (BioVendor) as per the manufacturer's specifications. Glomerulosclerotic index (GSI) was assessed in periodic acid–Schiff (PAS)-stained sections as previously described [20].

Transmission electron microscopy and analysis of mitochondrial morphology

Immediately following exsanguination, renal cortices were fixed in 2.5% glutaraldehyde in PBS for 4 h at room temperature. The samples were then rinsed three times in fresh buffer for 15 min each before post-fixing in 1% osmium tetroxide in buffer for 2 h at room temperature. Fixed tissue samples were rinsed three times in fresh buffer for 10 min each, before being dehydrated in increasing concentrations of ethanol consisting of 10, 30, 50, 70, 90, 100 and 100% anhydrous ethanol for 60 min each step. Following dehydration the cells were infiltrated with increasing concentrations of LR White resin in ethanol consisting of 25, 50, 75 and 100% resin for 6 h each step. After a second change of 100% resin the samples were embedded in fresh resin in gelatin capsules and allowed to sink to the bottom. The gelatin capsules were capped to exclude air and the resin was polymerized in an oven at 60 °C for 24 h. The embedded tissues in resin blocks were sectioned with a diamond knife on a Leica Ultracut S microtome and ultra-thin sections (90 nm) were collected on to formvar-coated 100 mesh hexagonal copper grids. The sections on grids were sequentially stained with 1% uranyl acetate for 10 min and Triple Lead Stain for 5 min [21] and viewed in a Phillips CM120 Biotwin transmission electron microscope at 120 kV. Images were captured with a Gatan Multiscan 600CW digital camera at a resolution of 1024 pixels × 1024 pixels. Ten images of proximal tubule epithelial cells (PTECs) per kidney section were randomly collected for each rat ($n = 5$ rats per group) at ×15 000 magnification. Mitochondrial length and width of all mitochondria within a given image (from ten images per rat) were measured using ImageJ (NIH) and the aspect ratio was calculated (length/width) and expressed as mean aspect ratio per group. In addition, mitochondrial roundness was evaluated using ImageJ within each field per section and expressed as mean mitochondrial roundness per group.

 © 2016 Authors; published by Portland Press Limited

Mitochondrial isolation

Mitochondria from fresh rat kidneys were isolated from 100 mg of renal cortex by differential centrifugation as previously described [22].

ATP

Mitochondrial ATP was measured using a bioluminescence ATP determination kit (Molecular Probes, Life Technologies) as described previously [23,24] with the following modifications. A ten-point standard curve was prepared, ranging from 50 000 nM to 125 nM. Data were normalized to citrate synthase activity and percentage control at the same time-point.

Citrate synthase activity

Citrate synthase activity was assayed as previously described [22].

Oxygen consumption rate

Oxygen consumption rates (OCRs) in isolated mitochondria from control and diabetic rats were measured using an Oxygraph-2 k high-resolution respirometer (Oroboros Instruments) [25].

Mitochondrial permeability transition

The induction of mitochondrial permeability transition (mPT) in rat kidney mitochondria was monitored by absorbance changes at 540 nm based on a microtitre plate procedure developed by Waldmeier et al. [26], with the following modifications. Rat kidney cortex obtained 10 min after death was homogenized in 5 mM HEPES containing 1 mM EGTA, 210 mM mannitol and 70 mM sucrose, pH 7.2. Mitochondria were isolated by differential centrifugation, washed twice and resuspended in energized respiratory buffer (210 mM mannitol, 70 mM sucrose, 5 mM glutamate, 5 mM malate, 0.05 M Tris/HCl and 5 mM H_3PO_4, pH 7.4). Mitochondrial protein (1 mg), was added to each well along with 82 μl of energized respiratory buffer and 10 μM cyclosporin A (CsA) where appropriate. At 5 min after the addition of CsA, 200 μM $CaCl_2 \cdot 2H_2O$ was added and the absorbance over 10 min was determined using a Wallac 1420 Victor^3 V Multilabel Counter (PerkinElmer).

Mitochondrial hydrogen peroxide production

Hydrogen peroxide (H_2O_2) production was measured in isolated mitochondria using the Amplex Red reagent as previously described [22].

Superoxide dismutase activity

The activity of superoxide dismutase in isolated mitochondria was assayed using the Cayman Chemical Company assay kit according to the manufacturer's instructions. Briefly, 10 μl of mitochondrial or cytosolic isolate, or standard, in duplicate was added to 200 μl of radical detector. The reaction was initiated by 20 μl of xanthine oxidase, incubated for 20 min at room temperature and the SOD activity was measured at 450 nm. Enzymatic activity was expressed as m-unit per mg of total protein.

15-Isoprostane F_{2t} ELISA

Urinary isoprostane excretion (15-isoprostane F_{2t}) was measured by a competitive ELISA specifically designed for urine (Oxford Biomedical Research), according to the manufacturer's instructions.

Western immunoblotting

Renal cortices were homogenized using a Next Advance Bullet Blender 24 at 4 °C, with 1.00 and 2.00 mm beads at speed 8 for 4 min in RIPA extraction buffer (10 mM Tris/HCl, pH 8.0, 150 mM sodium chloride, 1 % NP-40, 1 % sodium deoxycholate and 0.1 % SDS), containing Protease Inhibitor Cocktail (Roche) and Phosphatase Inhibitor Cocktail 2 (Sigma–Aldrich). The supernatant was obtained following centrifugation at 15 000 ***g*** for 15 min at 4 °C and protein content was determined using a BCA Protein Assay Kit (Pierce-Thermo Fisher Scientific). Immunoblotting was performed using β-actin (AC-15; 1:10 000 dilution) (Abcam) and rat monoclonal anti-OPA1 (GTPase optic atrophy-1; 1:1000 dilution, BD Transduction Laboratories).

Quantitative reverse transcription–PCR

RNA was isolated from kidney cortex (20–30 mg) using TRIzol Reagent (Life Technologies). DNA-free RNA was reverse-transcribed into cDNA using the Superscript First Strand Synthesis System according to the manufacturer's specifications (Life Technologies BRL). Real-time PCR was performed using SYBR Green PCR mixture (Applied Biosystems, primer concentration of 500 nM) using a 7500 Fast Real-Time PCR System (Applied Biosystem) and normalized relative to the 18S ribosomal RNA.

mtDNA copy number

DNA was extracted from renal cortex using a Maxwell 16 Instrument (Promega). DNA concentration was determined using a NanoDrop 1000 (Thermo Scientific). Mitochondrial DNA (mtDNA) copy number was determined by comparing the ratio of mtDNA to nuclear DNA (nDNA). Taqman primers and probes for POP5 (processing of precursor 5 gene; Rn02108253_s1, VIC-MGB, Applied Biosystems) was used as the nDNA reference gene. MT-CO3 (mitochondrially encoded cytochrome *C* oxidase III; Rn03296820_s1, FAM-MGB, Applied Biosystems) was used as the mtDNA reference gene. SDHA (succinate dehydrogenase complex, subunit A; Custom Reference #CCRR90D, NED-MGB, Applied Biosystems) a mitochondrial nuclear-encoded gene [mt(nDNA)] was used as an internal control. The three Taqman probes were multiplexed using a standard PCR run with TaqMan Master Mix (Applied Biosystems) and run on a 386-well QuantStudio 7 Flex System (Applied Biosystems). The ratios of mtDNA/nDNA and mt(nDNA)/nDNA was determined by comparing C_T values for each gene. PCR settings were denaturation at 95 °C for 10 min, 40 cycles of annealing at 95 °C for 15 s and extension at 60 °C for 1 min.

Statistics

All statistical computations were performed using Prism version 6.0 for Mac OS X (GraphPad Software). Values of experimental groups are given as mean, with bars showing the S.E.M., unless otherwise stated. Time and disease status (diabetes) effects were tested using two-way ANOVA with Bonferroni post-hoc analysis. $P < 0.05$ was considered to be statistically significant.

© 2016 Authors; published by Portland Press Limited

Table 1 Phenotypic and metabolic characteristics of rats
Data are means ± S.D., $n = 10$ per group. *$P < 0.0001$ compared with control at the same time-point.

	Body weight (g)	Kidney weight/body weight ($\times 10^{-3}$)	Blood glucose (mmol/l)	GHb (%)
Control 4 weeks	454 ± 17	6.9 ± 0.3	8.9 ± 1.1	4.4 ± 0.9
Diabetic 4 weeks	319 ± 47*	10.6 ± 0.6*	29.4 ± 4.4*	7.6 ± 1.4*
Control 8 weeks	451 ± 42	6.1 ± 0.3	8.6 ± 1.0	4.1 ± 1.1
Diabetic 8 weeks	295 ± 54*	10.5 ± 1.1*	30.5 ± 5.1	7.8 ± 1.0*
Control 16 weeks	517 ± 56	6.0 ± 1.0	7.6 ± 0.4	4.5 ± 0.2
Diabetic 16 weeks	374 ± 41*	10.5 ± 1.2*	26.6 ± 3.5*	6.6 ± 0.9*
Control 32 weeks	572 ± 30	5.8 ± 0.6	6.9 ± 0.8	4.2 ± 0.9
Diabetic 32 weeks	449 ± 21*	9.9 ± 1.3*	28.2 ± 2.9	7.8 ± 0.7*

RESULTS

Time-course of diabetic kidney disease

Body weight (BW) was decreased in diabetic rats compared with control rats at each time-point (Table 1). Kidney to BW ratio, blood glucose and GHb were each increased in diabetic animals compared with control within each time-point. Serum cystatin C, as a marker for glomerular filtration rate (Figure 1A), was decreased as early as 4 weeks after diabetes was established, indicating renal hyperfiltration, consistent with individuals with diabetes. Albuminuria had developed by 16 weeks of diabetes (Figure 1B) and this was preceded by glomerular morphological changes, glomerulosclerosis, which was apparent by week 8 of diabetes (Figures 1C and 1D). Significant tubular damage was evident by late diabetes (32 weeks) as reflected by an increase in urinary excretion of KIM-1 (Figure 1E).

Changes in mitochondrial bioenergetics precede development of renal structural injury and albuminuria

Mitochondrial bioenergetics were measured in freshly isolated mitochondria from kidney tissue (renal cortices). At 4 weeks of diabetes, mitochondrial ATP content was significantly decreased compared with control kidney, which persisted to 8 and 32 weeks of diabetes (Figure 2A). Although unchanged at weeks 4 and 8, mitochondrial respiration, assessed by OCR during both State III and uncoupled respiration in the presence of Complex I substrates glutamate and malate was increased at weeks 16 and 32 in diabetic kidneys (Figures 2B and 2C).

Enhanced susceptibility to mitochondrial permeability transition pore opening coincides with the development of renal morphological lesions

Freshly isolated mitochondria from renal cortices were exposed to vehicle, calcium (to induce pore opening) or calcium plus the mPT pore inhibitor CsA, and mPT pore opening (swelling) was assessed by light scattering at 450 nm. At 4 weeks after the development of diabetes, there was no change in mPT pore opening (Figure 3A). By 8 weeks of diabetes, there was an increased capacity for calcium-induced mPT pore opening, which persisted over the diabetes time-course (Figures 3B–3D). mPT pore opening was inhibited by CsA, an inhibitor of mPT (Figure 3D).

Both early and late diabetes are characterized by mitochondrial fragmentation

Next we explored mitochondrial morphology within PTECs, which constitute ~90% of the kidney cortex. Transmission electron microscopy showed mitochondria of a mixed population in PTECs in 4- and 32-week control kidney sections (Figure 4A, left), i.e. fragmented, intermediate and elongated. However, mitochondria in PTECs of diabetic rats were more fragmented (Figure 4A, right), at both 4 and 32 weeks of diabetes. This fragmented appearance was confirmed by assessment of mitochondrial aspect ratio, which takes into account both length and width, which was also decreased by diabetes at both time-points (Figure 4B). Mitochondrial roundness was also increased in the context of diabetes, further confirming a more fragmented phenotype in the diabetic kidney sections (Figure 4C).

Proteins involved in mitochondrial fission and fusion are altered throughout the time-course of diabetes in the kidney

Western immunoblotting of the protein OPA1 demonstrated that the long isoform 1 and 2 (L1 and L2) and three short isoforms (S1, S2 and S3) [27] were detected in both control and diabetic kidneys (Figures 5A–5F). The abundance of fusion-associated L1 and L2 were increased at 4 weeks of diabetes (Figures 5A and 5B), whereas only L1 was decreased at 32 weeks of diabetes (Figure 5A). The short isoforms are thought to regulate mitochondrial fission. There was no change in S1 (Figure 5C), but S2 was increased at week 16 (Figure 5D) and S3 by at 32 weeks of diabetes (Figure 5E). The gene expression of both mitofusin-1 (*Mfn1*) and mitofusin-2 (*Mfn2*), which regulate outer mitochondrial membrane fusion [28], were increased in the renal cortex of diabetic rats at 4 weeks of diabetes (Figures 5G and 5H respectively). Mitochondrial fission factor (*Mff*) expression was also up-regulated in early diabetes (Figure 5I).

The oxidative stress response is an early change in the diabetic kidney

Mitochondrial H_2O_2 production was increased at weeks 8, 16 and 32 of diabetes (Figure 6A). Manganese superoxide dismutase (MnSOD) activity, a key mitochondrial antioxidant enzyme, was suppressed from week 4 after diabetes and throughout diabetes duration (Figure 6B). Urinary excretion of 15-isoprostane F_{2t}, a marker of lipid peroxidation, was also increased early in

 © 2016 Authors; published by Portland Press Limited

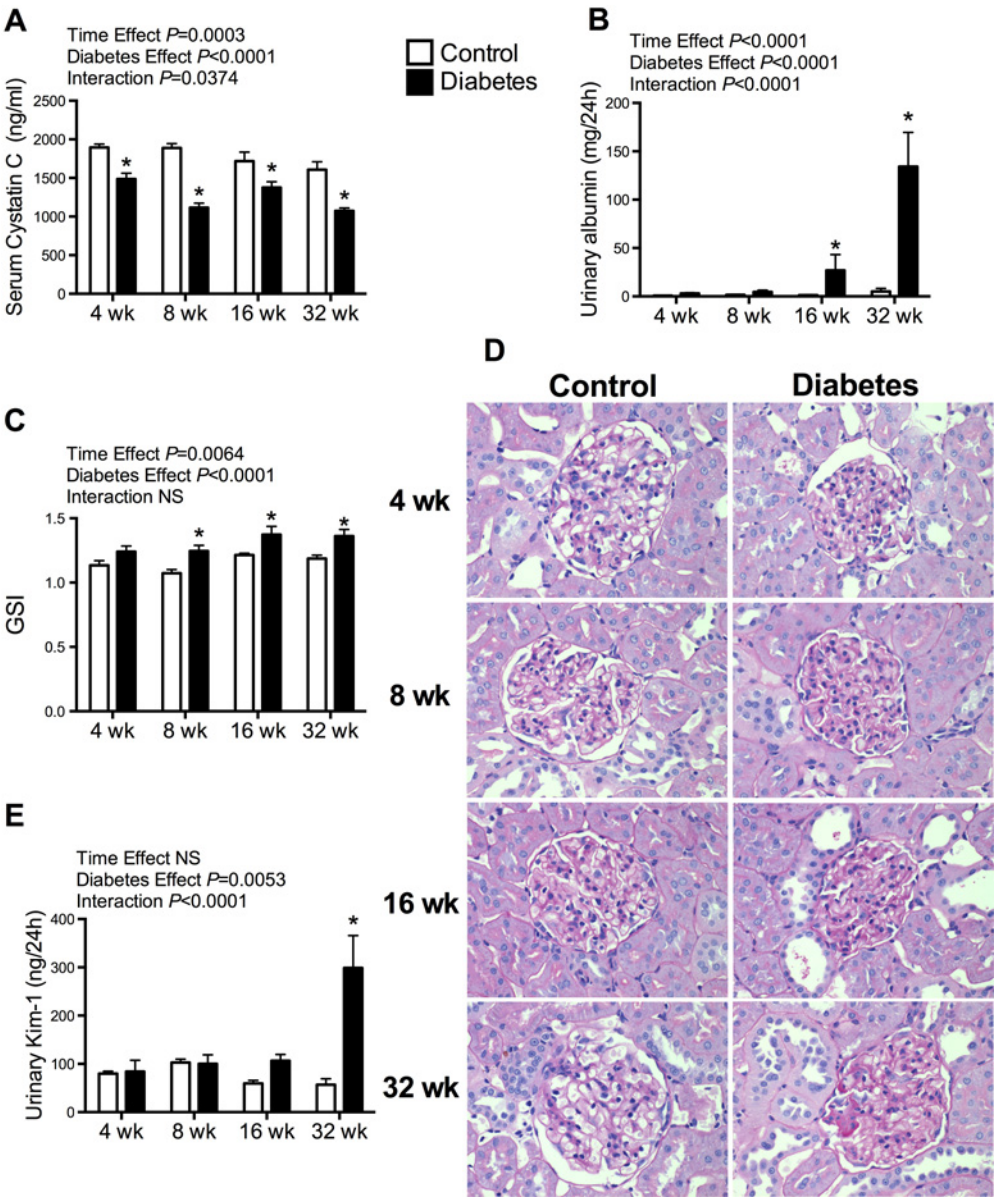

Figure 1 **Tracking development of the renal lesion in DKD**

(**A**) Serum cystatin C; (**B**) urinary albumin excretion; (**C**) GSI; (**D**) photomicrographs of PAS-stained renal cortex, ×400 magnification; (**E**) urinary excretion of KIM-1. Data are means ± S.E.M., $n = 10$ rats per group. *$P < 0.05$ compared with WT control at the same time-point.

diabetes, indicating an overall increase in oxidative stress status (Figure 6C).

Mitochondrial DNA copy number is increased in early diabetes

The ratio of mtDNA to nDNA was increased in the diabetic kidney at week 4 after diabetes (control, 0.75 ± 0.02 compared with diabetic, 0.78 ± 0.01; $P = 0.012$), but this did not persist to week 8, 16 or 32, with no effect over time on mtDNA copy number in either control rats or those with diabetes.

DISCUSSION

The present study has demonstrated that changes in mitochondrial bioenergetics and structure precede the development of albuminuria and renal structural defects in diabetes. As early as 4 weeks after diabetes induction, the ATP content within kidney mitochondria had decreased, and this was accompanied by the fragmentation of mitochondria, the increased expression of mitochondrial networking regulators OPA1 long isoforms, *Mfn1/2* and *Mff*, and an increase in mtDNA copy number and kidney hyperfiltration. Mitochondrial fragmentation was also associated with an increase in reactive oxygen species (ROS) generation.

© 2016 Authors; published by Portland Press Limited

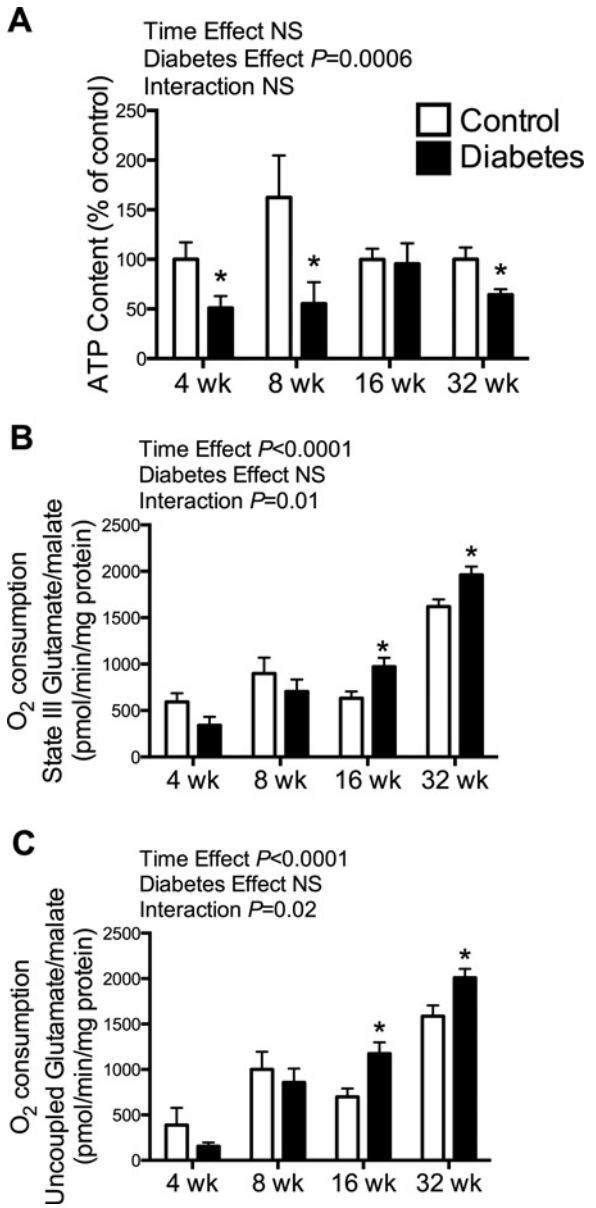

Figure 2 Changes in mitochondrial bioenergetics precede development of renal structural injury and albuminuria

Mitochondrial bioenergetics was measured in freshly isolated mitochondria from renal cortex. (**A**) Renal mitochondrial ATP; (**B**) State III Complex I-driven OCR; (**C**) uncoupled Complex I-driven OCR. Data are means ± S.E.M., $n = 5$ rats per group. $^*P < 0.05$ compared with WT control at the same time-point.

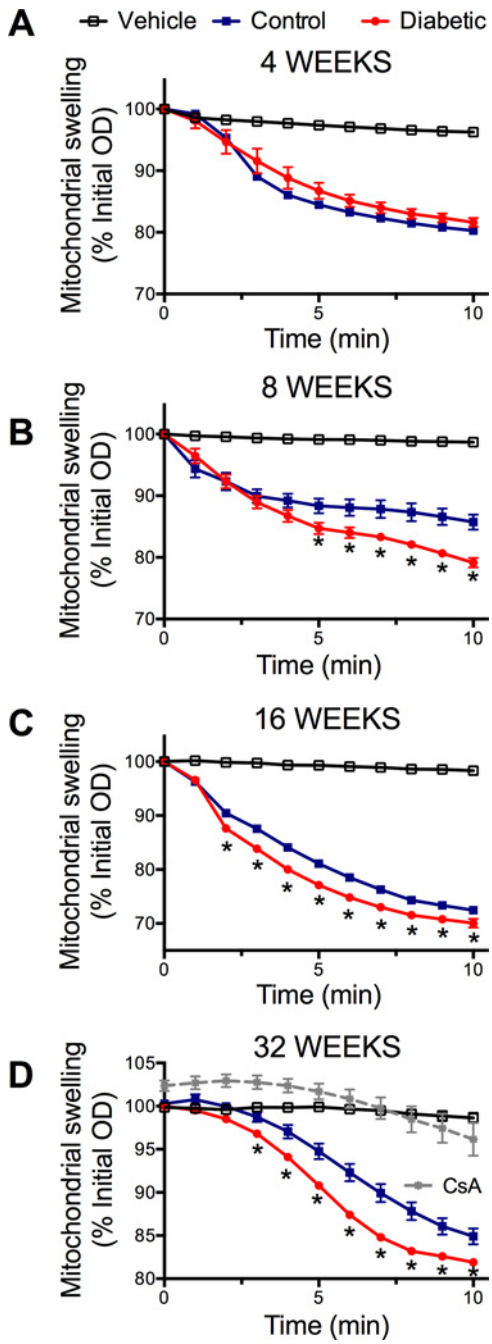

Figure 3 Increased susceptibility to mPT pore opening coincides with the development of renal morphological injury

Freshly isolated mitochondria from the renal cortex was exposed to vehicle, calcium (to induce pore opening) or calcium plus the mPT pore inhibitor CsA, and mPT pore opening (swelling) was assessed by light scattering at 450 nm. Data are expressed as percentage initial absorbance. Mitochondrial swelling in control compared with diabetic at (**A**) 4 weeks, (**B**) 8 weeks, (**C**) 16 weeks and (**D**) 32 weeks. Data are means ± S.E.M., $n = 5$ rats per group. $^*P < 0.05$ compared with WT control at the same time-point.

These mitochondrial defects persisted and by 16 weeks, when albuminuria and structural abnormalities had developed, there was evidence of a compensatory shift in State III and in uncoupled ATP production and mitochondrial dynamics, which restored kidney ATP content. However, by week 32 of diabetes, these compensatory mechanisms were not adequate to maintain kidney ATP concentrations, which were significantly decreased in line with the onset of tubular damage, marked by the increase in urinary KIM-1. Taken together, these data allude to mitochondrial abnormalities being primary initiators of DKD.

The kidneys are highly dependent on aerobic ATP production by OXPHOS in mitochondria [7] and at rest consume 7% of the

© 2016 Authors; published by Portland Press Limited

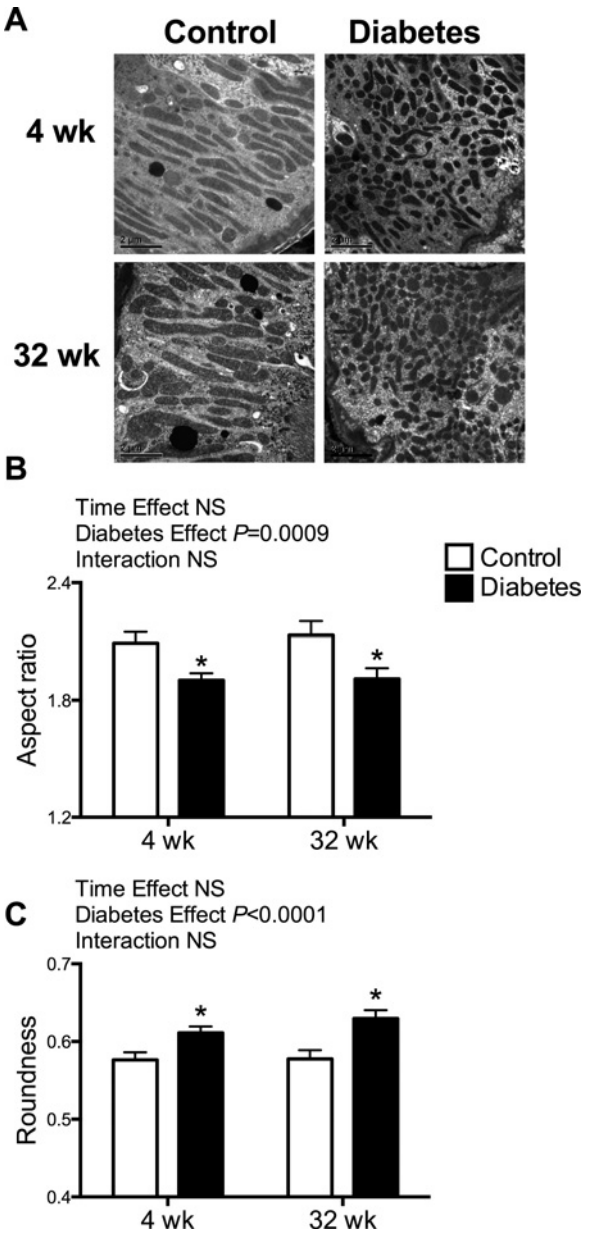

Figure 4 Proximal tubular cells show mitochondrial fragmentation early in diabetes which persists

(**A**) Electron micrographs of renal PTECs showing mitochondrial morphology in control (left) and diabetic (right) rats at 4 and 32 weeks. ×15 000 magnification. Scale bar = 2 μm. (**B**) Mitochondrial length and width were measured using ImageJ and aspect ratio was calculated (length/width). (**C**) Mitochondrial roundness was measured using ImageJ. Data are means ± S.E.M., $n = 10$ images per rat (with between 40 and 200 mitochondria scored in each image), $n = 5$ rats per group.

body's molecular oxygen [29]. Consistent with the present study, there is previous evidence that sustained hyperglycaemia results in increased kidney oxygen consumption, attributed to mitochondrial dysfunction [30]. In general, however, these studies show increased kidney oxygen consumption later in the progression of diabetic nephropathy, resulting in intra-renal tissue hypoxia, which is likely to be the result of an imbalance between increased oxygen consumption and delivery, leading to kidney fibrosis [30]. Interestingly, early kidney hyperfiltration at week 4 of the study may have increased oxygen delivery with diabetes and this was sustained for the duration of the study. We have also previously shown that a genetic mutation in the respiratory chain inducing mitochondrial dysfunction results in a decrease in kidney ATP content in the context of increased oxygen consumption and renal disease in adult mouse kidneys [22].

It has remained unclear, however, as to why in diabetes, the mitochondria are dysfunctional before oxygen consumption increases in the kidney. Indeed, in the present study, a decrease in kidney cortical ATP content was already evident by 4 weeks of diabetes, in the absence of increased mitochondrial oxygen consumption. Mitochondrial structure was also changed early in the development of DKD in our model, whereby mitochondria were fragmented and rounded at 4 weeks of diabetes. Fragmentation of mitochondria is a hallmark of ATP deficiency [31], in agreement with the decline in mitochondrial ATP content at the 4-week time-point of diabetes in the present study. There are other disorders where mitochondrial fragmentation and ATP loss are seen, such as in Huntington's disease where the early administration of agents that inhibit mitochondrial fission prevent tissue damage [32]. Similarly, inhibition of mitochondrial fission by overexpressing a fission mutant (DLP1-K38A) protects against diabetes-induced mitochondrial fission in proximal tubule cells and improves renal function [17].

The expression of key proteins involved in mitochondrial networking were also altered by 4 weeks of diabetes in the kidney. This included molecules associated with fission, *Mff*, as well as fusion, OPA1 long isoforms, *Mff1* and *Mff2*. However, given that electron microscopy analysis clearly revealed that mitochondrial fragmentation was present, mitochondrial fission was the predominating mitochondrial structural phenotype in early diabetes. It is puzzling as to why the fission phenotype has persisted in the kidney throughout the duration of the disease, despite, in general, a variation of mitochondrial networking molecules. This suggests that the drive for restoration of ATP content may be a more important signal for mitochondrial fission, rather than the fission of mitochondria driving ATP deficit. It should be noted that mDNA copy number was increased in early diabetes, suggesting induction of mitochondrial biogenesis at this time-point, but this was not sustained throughout diabetes duration. In the present study, the reasons for sustained mitochondrial fragmentation in the kidney remain unclear. However, it is possible that there is regulation of fission by other proteins which regulate mitochondrial dynamics such as parkin [33], and this may be driven by the search for alternative fuel sources [34]. Certainly, this is an area of great interest currently and warrants further investigation in DKD.

There was also a sustained increase in the generation of renal cortical H_2O_2 from mitochondria from rats with diabetes, which could have been responsible for the mitochondrial fragmentation observed in the PTECs. Indeed, imbalances in mitochondrial ROS production are a recognized stimulus for mitochondrial fragmentation [33]. It is also conceivable that the increases in ROS leading to mitochondrial fragmentation are the result of increases in NADPH oxidase activity which are characteristic of the diabetic kidney [9], although this was not assessed in the present study.

© 2016 Authors; published by Portland Press Limited

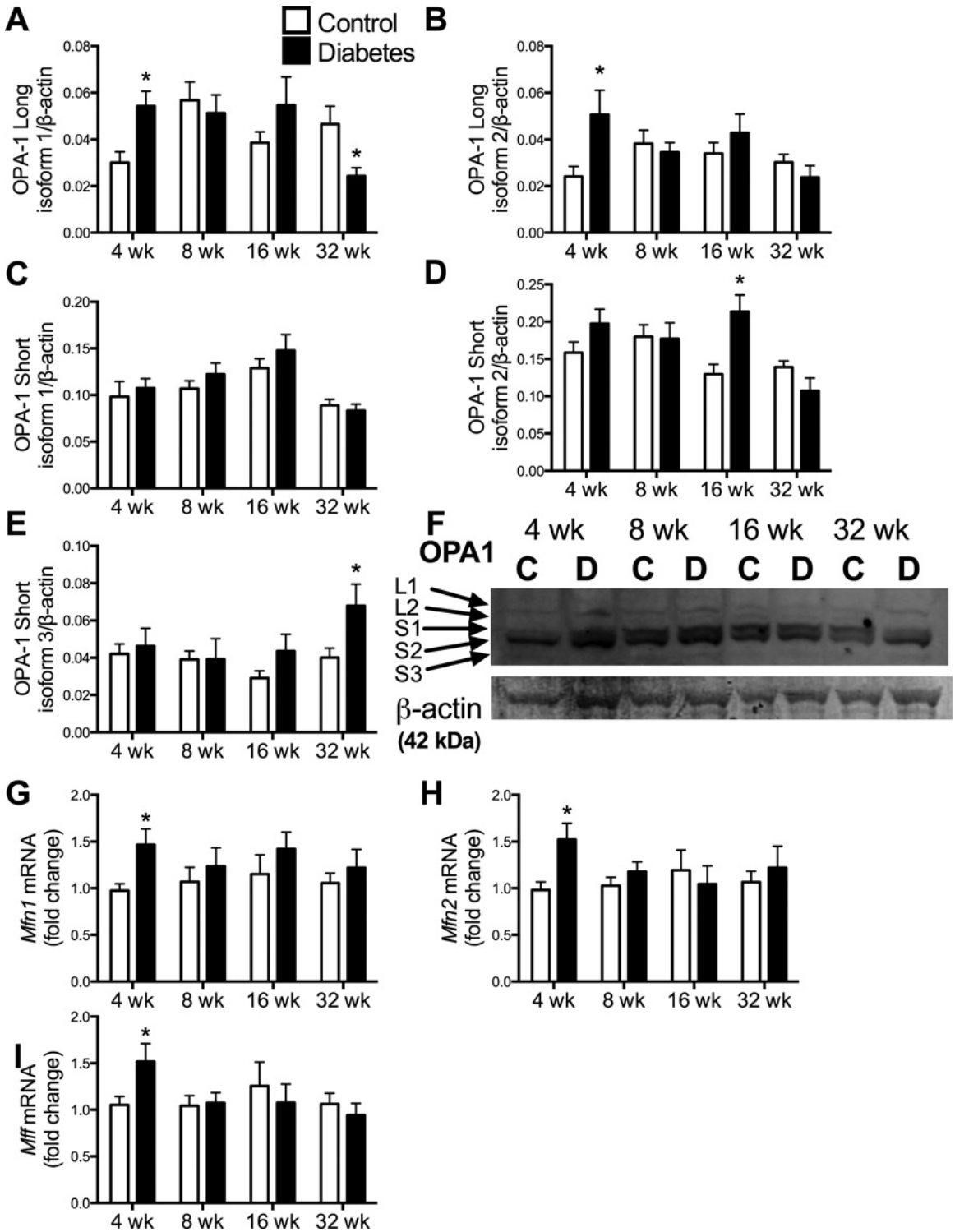

Figure 5 Proteins involved in mitochondrial fission and fusion are altered throughout the time-course of diabetes

Quantification of OPA1 Western blot, $n = 6$ rats per group. (**A**) OPA1 long isoform 1; (**B**) OPA1 long isoform 2; (**C**) OPA1 short isoform 1; (**D**) OPA1 short isoform 2; (**E**) OPA1 short isoform 2. (**F**) Representative Western blot (gradient gel) of OPA1 in showing the five isoforms: long isoforms 1 and 2 (L1 and L2) and short isoforms 1–3 (S1, S2 and S3) (spanning 80–100 kDa). β-Actin loading control (42 kDa, bottom). C, control; D, diabetic. (**G**–**J**) Quantitative PCR analysis of genes involved in mitochondrial dynamics in renal cortex (**G**) *Mfn1*, (**H**) *Mfn2*, (**I**) *Mff*; $n = 10$ rats per group.

© 2016 Authors; published by Portland Press Limited

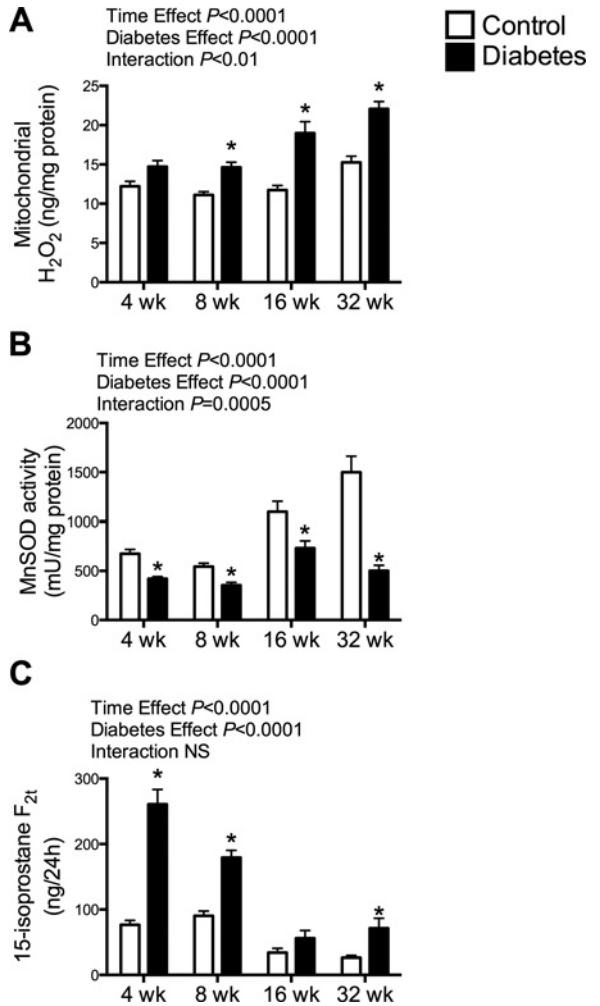

Figure 6 Oxidative stress response is up-regulated in diabetic nephropathy

(**A**) Mitochondrial H_2O_2 production; (**B**) MnSOD activity; (**C**) urinary excretion of 15-isoprostane F_{2t}. Data are means ± S.E.M., $n = 5$–10 rats per group. *$P < 0.05$ compared with WT control at the same time-point.

Diabetes-induced increases in the generation of H_2O_2 have also been shown to lead to mPT opening [8] as seen in the present study. It is likely that the increase in mPT, i.e. opening of the mPT pore, could also contribute to the decrease in ATP content observed in the diabetic kidneys, since it is a trafficking site for ADP and ATP between the cytosol and mitochondria. Furthermore, the mPT opening was induced in the presence of calcium which is a stimulus known to be altered in the diabetic milieu [33] by processes such as endoplasmic reticulum stress.

Overall, the present study postulates that defects in mitochondrial function are primary initiators of kidney disease in diabetes. Mitochondrial fragmentation and ATP loss were seen with diabetes before evidence of renal injury was present. Furthermore, the evidence indicates that excess ROS generation and increased susceptibility to mPT were more tightly linked to the changes in mitochondrial morphology and function, rather than sustained changes in typical mitochondrial networking proteins. Hence, kidney function in diabetes may be improved by strategies to prevent mitochondrial dysfunction and this should be an area of prioritized research effort in the future for this disease.

CLINICAL PERSPECTIVES

- Mitochondrial dysfunction is seen at sites of diabetes complications including in the kidneys.
- We hypothesized that mitochondrial dysfunction is an early event in the pathogenesis of DKD.
- The present study showed that mitochondrial dysfunction precedes kidney dysfunction in diabetes and hence may be a primary cause of diabetic nephropathy able to be therapeutically targeted to prevent this disease.

AUTHOR CONTRIBUTION

Melinda Coughlan ran the animal studies, researched the data and co-wrote the paper. Tuong-Vi Nguyen, Sally Penfold, Gavin Higgins, Vicki Thallas-Bonke, Sih Tan, Nicole Van Bergen, Karly Sourris, Brooke Harcourt, David Thorburn, Ian Trounce and Mark Cooper researched the data. Josephine Forbes conceived the studies, researched the data and co-wrote the paper.

ACKNOWLEDGEMENTS

We thank Amy Morley, Felicia Yap, Anna Gasser and Maryann Arnstein for their technical expertise. We also thank Dr Simon Crawford (University of Melbourne) for assistance with electron microscopy.

FUNDING

This work was supported by the Juvenile Diabetes Research Foundation (JDRF) [grant number 3-PDF-2014-106-A-N (to G.C.H.)]; the National Health and Medical Research Council of Australia (NHMRC) [grant numbers GNT1023664, GNT1004503, GNT1078808, and GNT1022896 (to J.M.F., D.R.T. and M.E.C.)]; the Mater Foundation; the Victorian Government's Operational Infrastructure Support Program; the Australian and New Zealand Society of Nephrology Career Development Fellowship (to M.T.C.)].

REFERENCES

1 Go, A.S., Chertow, G.M., Fan, D., McCulloch, C.E. and Hsu, C.Y. (2004) Chronic kidney disease and the risks of death, cardiovascular events, and hospitalization. N. Engl. J. Med. **351**, 1296–1305 CrossRef PubMed

2 Lysaght, M.J. (2002) Maintenance dialysis population dynamics: current trends and long-term implications. J. Am. Soc. Nephrol. **13** (Suppl. 1), S37–S40 PubMed

3 Couser, W.G., Remuzzi, G., Mendis, S. and Tonelli, M. (2011) The contribution of chronic kidney disease to the global burden of major noncommunicable diseases. Kidney Int. **80**, 1258–1270 CrossRef PubMed

© 2016 Authors; published by Portland Press Limited

4 Collins, A.J., Foley, R.N., Herzog, C., Chavers, B., Gilbertson, D., Ishani, A., Kasiske, B., Liu, J., Mau, L.W., McBean, M. et al. (2009) United States Renal Data System 2008 Annual Data Report. Am. J. Kidney Dis. **53** (Suppl.), S1–S374 PubMed

5 Palmer, N.D. and Freedman, B.I. (2012) Insights into the genetic architecture of diabetic nephropathy. Curr. Diab. Rep. **12**, 423–431 CrossRef PubMed

6 Brenner, B.M., Cooper, M.E., de Zeeuw, D., Keane, W.F., Mitch, W.E., Parving, H.H., Remuzzi, G., Snapinn, S.M., Zhang, Z. and Shahinfar, S. (2001) Effects of losartan on renal and cardiovascular outcomes in patients with type 2 diabetes and nephropathy. N. Engl. J. Med. **345**, 861–869 CrossRef PubMed

7 Soltoff, S.P. (1986) ATP and the regulation of renal cell function. Annu. Rev. Physiol. **48**, 9–31 CrossRef PubMed

8 Coughlan, M.T., Thorburn, D.R., Penfold, S.A., Laskowski, A., Harcourt, B.E., Sourris, K.C., Tan, A.L., Fukami, K., Thallas-Bonke, V., Nawroth, P.P. et al. (2009) RAGE-induced cytosolic ROS promote mitochondrial superoxide generation in diabetes. J. Am. Soc. Nephrol. **20**, 742–752 CrossRef PubMed

9 Forbes, J.M., Coughlan, M.T. and Cooper, M.E. (2008) Oxidative stress as a major culprit in kidney disease in diabetes. Diabetes **57**, 1446–1454 CrossRef PubMed

10 Sharma, K., Karl, B., Mathew, A.V., Gangoiti, J.A., Wassel, C.L., Saito, R., Pu, M., Sharma, S., You, Y.H., Wang, L. et al. (2013) Metabolomics reveals signature of mitochondrial dysfunction in diabetic kidney disease. J. Am. Soc. Nephrol. **24**, 1901–1912 CrossRef PubMed

11 Sivitz, W.I. and Yorek, M.A. (2010) Mitochondrial dysfunction in diabetes: from molecular mechanisms to functional significance and therapeutic opportunities. Antioxid. Redox Signal. **12**, 537–577 CrossRef PubMed

12 Daehn, I., Casalena, G., Zhang, T., Shi, S., Fenninger, F., Barasch, N., Yu, L., D'Agati, V., Schlondorff, D., Kriz, W. et al. (2014) Endothelial mitochondrial oxidative stress determines podocyte depletion in segmental glomerulosclerosis. J. Clin. Invest. **124**, 1608–1621 CrossRef PubMed

13 Che, R., Yuan, Y., Huang, S. and Zhang, A. (2014) Mitochondrial dysfunction in the pathophysiology of renal diseases. Am. J. Physiol. Renal Physiol. **306**, F367–F378 CrossRef PubMed

14 Hall, A.M. and Unwin, R.J. (2007) The not so 'mighty chondrion': emergence of renal diseases due to mitochondrial dysfunction. Nephron Physiol. **105**, 1–10 CrossRef PubMed

15 Rosca, M.G., Mustata, T.G., Kinter, M.T., Ozdemir, A.M., Kern, T.S., Szweda, L.I., Brownlee, M., Monnier, V.M. and Weiss, M.F. (2005) Glycation of mitochondrial proteins from diabetic rat kidney is associated with excess superoxide formation. Am. J. Physiol. Renal Physiol. **289**, F420–F430 CrossRef PubMed

16 Wang, W., Wang, Y., Long, J., Wang, J., Haudek, S.B., Overbeek, P., Chang, B.H., Schumacker, P.T. and Danesh, F.R. (2012) Mitochondrial fission triggered by hyperglycemia is mediated by ROCK1 activation in podocytes and endothelial cells. Cell Metab. **15**, 186–200 CrossRef PubMed

17 Galloway, C.A., Lee, H., Nejjar, S., Jhun, B.S., Yu, T., Hsu, W. and Yoon, Y. (2012) Transgenic control of mitochondrial fission induces mitochondrial uncoupling and relieves diabetic oxidative stress. Diabetes **61**, 2093–2104 CrossRef PubMed

18 Zhan, M., Usman, I.M., Sun, L. and Kanwar, Y.S. (2015) Disruption of renal tubular mitochondrial quality control by myo-inositol oxygenase in diabetic kidney disease. J. Am. Soc. Nephrol. **26**, 1304–1321 CrossRef PubMed

19 Coughlan, M.T. and Forbes, J.M. (2011) Temporal increases in urinary carboxymethyllysine correlate with albuminuria development in diabetes. Am. J. Nephrol. **34**, 9–17 CrossRef PubMed

20 Saito, T., Sumithran, E., Glasgow, E.F. and Atkins, R.C. (1987) The enhancement of aminonucleoside nephrosis by the co-administration of protamine. Kidney Int. **32**, 691–699 CrossRef PubMed

21 Sato, T. (1968) A modified method for lead staining of thin sections. J. Electron Microsc. (Tokyo) **17**, 158–159 PubMed

22 Forbes, J.M., Ke, B.X., Nguyen, T.V., Henstridge, D.C., Penfold, S.A., Laskowski, A., Sourris, K.C., Groschner, L.N., Cooper, M.E., Thorburn, D.R. et al. (2013) Deficiency in mitochondrial Complex I activity due to Ndufs6 gene trap insertion induces renal disease. Antioxid. Redox Signal. **19**, 331–343 CrossRef PubMed

23 Coughlan, M.T., Yap, F.Y., Tong, D.C., Andrikopoulos, S., Gasser, A., Thallas-Bonke, V., Webster, D.E., Miyazaki, J., Kay, T.W., Slattery, R.M. et al. (2011) Advanced glycation end products are direct modulators of beta-cell function. Diabetes **60**, 2523–2532 CrossRef PubMed

24 Drew, B. and Leeuwenburgh, C. (2003) Method for measuring ATP production in isolated mitochondria: ATP production in brain and liver mitochondria of Fischer-344 rats with age and caloric restriction. Am. J. Physiol. Regul. Integr. Comp. Physiol. **285**, R1259–R1267 CrossRef PubMed

25 Lee, S., Sheck, L., Crowston, J.G., Van Bergen, N.J., O'Neill, E.C., O'Hare, F., Kong, Y.X., Chrysostomou, V., Vincent, A.L. and Trounce, I.A. (2012) Impaired complex-I-linked respiration and ATP synthesis in primary open-angle glaucoma patient lymphoblasts. Invest. Ophthalmol. Vis. Sci. **53**, 2431–2437 CrossRef PubMed

26 Waldmeier, P.C., Feldtrauer, J.J., Qian, T. and Lemasters, J.J. (2002) Inhibition of the mitochondrial permeability transition by the nonimmunosuppressive cyclosporin derivative NIM811. Mol. Pharmacol. **62**, 22–29 CrossRef PubMed

27 Anand, R., Wai, T., Baker, M.J., Kladt, N., Schauss, A.C., Rugarli, E. and Langer, T. (2014) The i-AAA protease YME1L and OMA1 cleave OPA1 to balance mitochondrial fusion and fission. J. Cell Biol. **204**, 919–929 CrossRef PubMed

28 Westermann, B. (2010) Mitochondrial fusion and fission in cell life and death. Nat. Rev. Mol. Cell Biol. **11**, 872–884 CrossRef PubMed

29 Valtin, H. (1983) Renal Function: Mechanisms Preserving Fluid and Solute Balance in Health, Little Brown, Boston

30 Friederich-Persson, M., Thorn, E., Hansell, P., Nangaku, M., Levin, M. and Palm, F. (2013) Kidney hypoxia, attributable to increased oxygen consumption, induces nephropathy independently of hyperglycemia and oxidative stress. Hypertension **62**, 914–919 CrossRef PubMed

31 Knott, A.B., Perkins, G., Schwarzenbacher, R. and Bossy-Wetzel, E. (2008) Mitochondrial fragmentation in neurodegeneration. Nat. Rev. Neurosci. **9**, 505–518 CrossRef PubMed

32 Guo, X., Disatnik, M.H., Monbureau, M., Shamloo, M., Mochly-Rosen, D. and Qi, X. (2013) Inhibition of mitochondrial fragmentation diminishes Huntington's disease-associated neurodegeneration. J. Clin. Invest. **123**, 5371–5388 CrossRef PubMed

33 Higgins, G.C. and Coughlan, M.T. (2014) Mitochondrial dysfunction and mitophagy: the beginning and end to diabetic nephropathy? Br. J. Pharmacol. **171**, 1917–1942 CrossRef PubMed

34 Guido, C., Whitaker-Menezes, D., Lin, Z., Pestell, R.G., Howell, A., Zimmers, T.A., Casimiro, M.C., Aquila, S., Ando, S., Martinez-Outschoorn, U.E. et al. (2012) Mitochondrial fission induces glycolytic reprogramming in cancer-associated myofibroblasts, driving stromal lactate production, and early tumor growth. Oncotarget **3**, 798–810 CrossRef PubMed

Received 26 November 2015/14 January 2016; accepted 1 February 2016

Accepted Manuscript online 1 February 2016, doi: 10.1042/CS20150838

 © 2016 Authors; published by Portland Press Limited